Received: 17 September 2024 | Revised: 14 January 2025 | Accepted: 16 February 2025

DOI: 10.1002/mp.17743

RESEARCH ARTICLE

MEDICAL PHYSICS

Quantifying the dosimetric accuracy of expiration-gated stereotactic lung radiotherapy

Daan Hoffmans[1,2] | **Isabel Remmerts de Vries**[1] | **Max Dahele**[1] | **Wilko Verbakel**[1,3]

[1]Department of Radiation Oncology, Amsterdam UMC location Vrije Universiteit Amsterdam, Amsterdam, The Netherlands

[2]Cancer Center Amsterdam, Cancer Treatment and Quality of Life, Amsterdam, The Netherlands

[3]Varian Medical Systems, Radiotherapy Solutions, Palo Alto, USA

Correspondence
Daan Hoffmans, Amsterdam UMC location Vrije Universiteit Amsterdam, Department of Radiation Oncology, De Boelelaan 1117, 1081HV Amsterdam, The Netherlands.
Email: d.hoffmans@amsterdamumc.nl

Abstract

Background: In stereotactic body radiotherapy, a form of motion management is often applied to mobile lung tumors. Gated radiotherapy is such form of motion management in which the radiation beam is switched on or off depending on the actual tumor position. Compared to inspiration, the tumor position is typically more stable during expiration. Also, the tumor spends more time in expiration position. Therefore, we often consider expiration-gating for patients with relatively large tumor motion.

Purpose: We validated dosimetric accuracy of expiration-gated stereotactic lung radiotherapy by means of phantom measurements and modeling the effects of residual motion in patients.

Methods: Dose profiles from film measurements in a respiratory-motion phantom were compared to dose calculations, for different expiration gating methods. Fluoroscopic real-time tumor tracking was used to produce a convolution kernel which was applied to the calculated dose distribution to model dosimetric effects of residual motion. This convolution method was validated against film measurements and then retrospectively applied to clinical tumor tracking data of five patients. In addition, clinical tumor motion data was manipulated to simulate the effect of a short breathing period of 2 s and prolonged gating latency of 500 ms.

Results: A good agreement between calculated and measured dose was found when amplitude gating was used (100% gamma pass rate, 3%/2 mm). For phase gating, good agreement required a stable breathing period. Measurements showed good performance of the convolution method (gamma pass rate $>$ 99%). For the clinical data, we found a maximal dose shift of 2.4 mm, introduced by residual tumor motion or respiratory drift. For all patients, the size of the ITV was adequate to account for this dose shift. Simulating higher breathing speed in combination with large latency values resulted in dosimetric shifts that were larger than the PTV margin.

Conclusion: Amplitude gating is robust for irregular breathing patterns. Expiration-gating is a dosimetrically accurate method of treatment delivery provided that during delivery there is a prompt reaction to respiratory drift and the latency of the gating system is short.

KEYWORDS
exhale gating, expiration gating, residual motion, tumor tracking

1 | INTRODUCTION

Stereotactic body radiotherapy (SBRT) for lung tumors is often performed in free-breathing, irradiating an internal target volume (ITV) that incorporates the entire range of motion detected on an uncoached four-dimensional CT (4DCT)-scan. Above a certain motion threshold, many treating teams will choose to use a motion management technique; although AAPM report 91 suggested a threshold of 5 mm,[1] in practice this often depends on tumor position and location.[2] Gated treatment, that is, irradiation only during certain breathing phases, is one approach to respiratory management. The most common form is deep inspiration breath hold (DIBH), but this has the disadvantage that patients need to be fit enough to perform multiple breath-holds and large inter-breath hold variation of the tumor position has occasionally been observed.[3,4]

While inspiration gating could lead to better sparing of healthy lung tissue than expiration gating due to the larger lung volume in inspiration,[5] the intra-fraction variability of the respiration amplitude is smallest in the expiration phases resulting in higher geometric precision for expiration/exhale gating.[6,7] In addition, during free-breathing, tumors generally spend a longer time in expiration phases than in inhale phases, resulting in shorter treatment times.[5]

For these reasons, in our clinic, lung tumors with a relatively large motion amplitude (typically, but not exclusively, $>$ 10 mm) may be considered for SBRT in expiration-gating. For a minority of these patients, we tracked the tumor position in real-time.[3,8,9]

The expiration-gating period is derived from selected expiration phases of a 10-phase 4DCT-scan, typically the 30 or 40%–70% phases; these are translated to amplitude thresholds for a reflective marker block placed on the surface of the upper abdomen (Respiratory Gating for Scanners, RGSC, Varian a Siemens Healthineers company, Palo Alto, USA), the motion of which is tracked during breathing. The relationship between the RGSC block and the breathing phase is determined during the 4DCT scan, and if this relative relationship does not change, it is assumed to be indicative for the position of the mobile tumor. However, the relationship between the external gating signal (marker block position) and the internal tumor position might change during or between fractions: for example, variation in expiration position, breathing depth and frequency during a treatment fraction and relaxation of the patient from fraction to fraction.[10–12] Because the gating system does not quantitatively update the relationship between the position of the marker block and the tumor, these changes in the relationship between the external gating signal and the tumor lead to an unknown amount of uncertainty in the process. An attempt is made to account for this by using a PTV (planning target volume) margin around the expiration-gating ITV (internal target volume). If this PTV margin is inadequate, part of the tumor may be outside the PTV for part of the time, leading to underdosage of the tumor and unnecessary irradiation of healthy lung tissue. Besides these patient-related factors, technical properties of the radiotherapy equipment can also affect the accuracy of gated dose delivery. The beam has to be switched on or off when the gating thresholds are passed—suffering from beam latency.[13] The latency may include factors such as the refresh rate of the respiratory monitoring system, data processing and communication between the gating system and the linear accelerator. A wide variety of gating latencies are reported ranging from 45 to 100 milliseconds (ms) for Varian TrueBeam linear accelerators using the integrated gating system.[14–16] Larger values up to 800 ms are reported when using dedicated surface guidance (SGRT) systems.[16,17] In addition, there can be a delay between the actual movement of a tumor outside of the PTV and the motion of the surrogate (e.g., surface of the patient). The introduction of unforeseen residual tumor motion during the beam-on window, secondary to patient-related and/or technical factors might impact the dosimetric accuracy of gated dose delivery.

To estimate the dosimetric effect of target motion during treatment, a convolution with motion can be used.[18,19] Although such a convolution method is verified by phantom measurements,[20,21] application to data collected during patient treatment is restricted to treatment sites such as liver or prostate where fiducial markers were used for tumor tracking during un-gated radiotherapy.[22–25]

In this research, we used the tumor position measured by markerless intrafraction real-time kV tracking during expiration-gated lung SBRT[3,8,9] to determine a convolution kernel for estimation of the dosimetric effect of residual motion in expiration-gating and we verified the method with film measurements. Then, we applied this convolution method to clinical data to assess the impact of individual elements such as drift, latency, and breathing speed. Finally, we test whether the volume of the ITV is sufficient to account for tumor motion within the gating window.

2 | METHODS

2.1 | Clinical workflow

For lung SBRT patients treated in expiration gating, a 4DCT-scan is acquired (Discovery CT590 RT, General Electric, Boston, USA) during uncoached free-breathing. During CT acquisition, the respiratory waveform is registered by the RGSC system that tracks a marker block positioned on the surface of the upper abdomen of the patient, caudally of the sternum. Based on this

waveform, the CT is reconstructed in 10 phase bins of which the 50% bin represents end-expiration. For target delineation and treatment planning, an average intensity projection CT (CT_{ave}) is made of the expiration phase bins that contain minimal tumor motion (typically 30 or 40%–70%). An ITV is contoured using the selected expiration phases of the 4DCT-scan, and the PTV is generally formed by a 5 mm isotropic expansion of the ITV (occasionally 3 mm). The treatment mode with maximum dose rate is chosen in order to minimize the treatment time per fraction and fastest delivery during the short gate windows. Therefore, a multiple (partial) arc 10 MV flattening filter free (FFF) VMAT plan, with a maximum dose rate of 2400 MU/min is made in Eclipse (Varian, version 16.1.0) with 95% of the PTV receiving the prescribed dose and a Dmax < 140% located in the ITV. Dose was calculated using Acuros (Varian, version 16.1). The plan typically focuses on keeping the lung dose as low as possible.

On the treatment machine (TrueBeam version 2.7, Varian), a marker block identical to the one used by RGSC, on the same position as during the CT-scan, is tracked by the integrated real-time position management (RPM) system. In terms of accuracy and efficiency, amplitude gating is demonstrated to be superior to phase gating.[7,26,27] Therefore, amplitude gating is used instead of phase gating. The approximate RPM waveform amplitude range corresponding to the selected breathing phases from the 4DCT-scan is used as gating threshold during treatment. The included expiration phases often correspond to an RPM upper threshold of approximately 3 mm, but this threshold could differ dependent on the patients individual breathing waveform. The 50% expiration should correspond to an RPM position of 0, but to accept a bit of variation in the baseline, a lower threshold of -2 or -3 mm is often used. Although the begin-expiration and end-expiration could require different upper thresholds, only one threshold can be selected, which may lead to undesired residual breathing motion of the tumor within the gating window.

First, a gated cone beam computed tomography (CBCT) scan is made for online setup correction based on tumor matching. Then, treatment delivery was performed under uncoached free-breathing expiration gating conditions. For some of the fractions, delivery was combined with 7 frames per second (FPS) fluoroscopy. The fluoroscopic images were used to track the actual tumor position using RapidTrack Realtime (RTR), a non-clinical software system running fully independently from the clinical workflow. This software detects the two-dimensional tumor position in the fluoroscopic images by using template matching by normalized cross-correlation and calculates the three-dimensional tumor position using triangulation with previous fluoroscopic images acquired from a different gantry angle.[9]

2.2 | Measurements

Film (GafChromic EBT3, Asland) measurements were performed to assess the dosimetric effect of residual motion during expiration gating. Using the Quasar Respiratory Motion Phantom (Modus QA)[28,29] with a wooden insert that contains a plastic sphere representing a tumor, various simulated scenarios such as amplitude gating and phase gating for a constant- and varying breathing speed were measured. Also, the effects of very high breathing speed, and erroneous choice of the gating window were measured.

Three motion patterns with a peak-to-peak amplitude of 30 mm were generated, mimicking a worst-case scenario. Two patterns simulated regular breathing with periods of 5 and 2 s, the third pattern simulated a varying breathing period within the range of 2–8 s (Figure 1). Using the regular motion pattern with the 5-s period, we acquired a 4DCT-scan of the QUASAR phantom and constructed a CT_{ave} from phase bins 40–70 spanning the expiration period of the motion pattern. Then, CT_{ave} was used to delineate an ITV, which was isotropic expanded by 5 mm to a PTV. A 2-full arc 10 MV FFF VMAT plan was created to deliver a fraction dose of 7.5 Gy to 95% of the PTV and a Dmax < 10.5 Gy in the ITV. In order to stay within the dose range where we experienced the best accuracy and reproducibility of GafChromic film, the number of monitor units of the plan was halved. To maintain the original dynamics of in terms of treatment time and velocity of the MLC and gantry, the maximum dose rate of the plan was also halved to 1200 MU/min.

On the treatment machine, the phantom was aligned using an amplitude gated CBCT, while the phantom was performing the regular breathing pattern with 5-s period. Once aligned, we performed seven measurements: (a) measurement 1 and 2: amplitude gating with the regular and irregular breathing pattern, respectively, (b) measurement 3 and 4: phase gating with the regular and irregular breathing pattern respectively, (c) measurement 5: regular breathing pattern, but with the upper- and lower phase gating thresholds swapped from 35%–75% to 75%–35% (note that the 40% phase bin contains data from 35% to 45%), resulting in the beam being turned on around inhalation and excessive motion within the gating window, (d) measurement 6: amplitude gating with the 2-s breathing period. This was to investigate a possible effect of the gating latency, which could become more prominent for smaller periods, (e) measurement 7: a stationary phantom with the target at expiration 0.0 mm position was re-aligned using an un-gated CBCT, and then, the plan was delivered to the stationary target to determine the measurement precision.

During delivery, the sphere position was tracked using RTR, and the RPM signal (the motion waveform of the

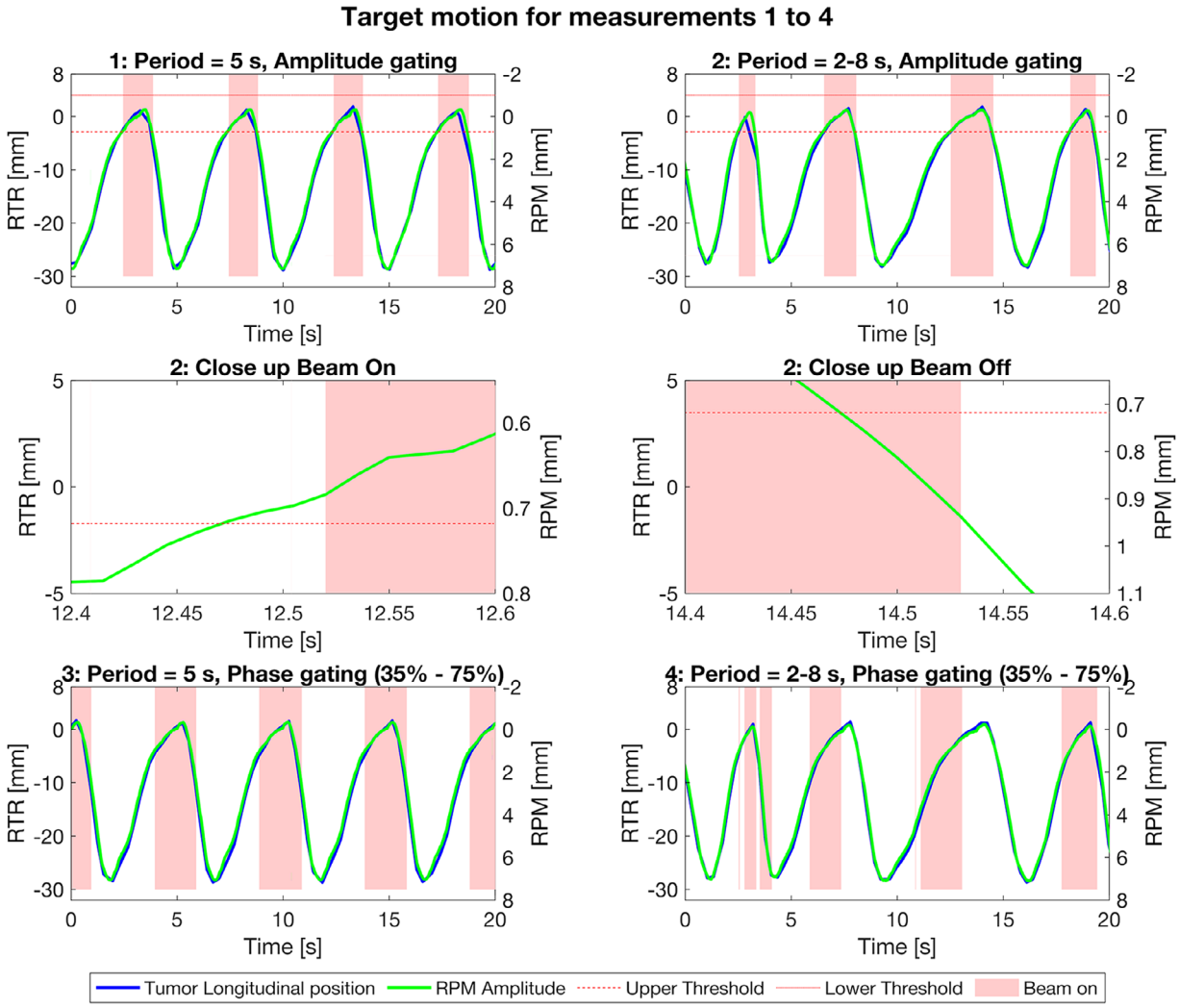

FIGURE 1 Motion traces for the film measurements. The sphere position as tracked by rapid track real-time (RTR), the corresponding real-time position management (RPM) signal. Beam-on intervals are marked in red. Two close-up windows for measurement 2 show the apparent latency: the time difference between the moment the RPM signal crosses the amplitude threshold and the beam-status transition.

marker block) was stored in Aria (Varian Medical Systems, version 16.00.00). After plan delivery, the films were digitized and converted to absolute dose using in-house developed Matlab (Mathworks, R2018b) software. Longitudinal dose profiles were extracted from the measurements and the dose calculation.

2.3 | Modeling of measured dosimetric effects

The motion waveform data contained the motion amplitude of the external marker block with a time resolution of 15 ms and the timestamps at which the beam was switched on and off. The external marker amplitude signal is also present in the RTR data. This meant it was possible to align the time axis of the RPM signal to that of the RTR data. The RTR data has a time resolution of 140 ms, which was linearly interpolated to the time axis of the RPM signal. The apparent beam-on and beam-off latency in these data was assessed by quantifying the time between the RPM signal crossing the amplitude boundary and the beam transition time recorded in the RPM export file. We did this for all beam-transitions of the first arc of measurement 2 and calculated mean value and its standard deviation (SD). Then, two position histograms were calculated in which the target position was distributed over 0.25 mm bins. The first histogram contained the tumor positions at moments of beam-off, the second histogram contained the tumor position at beam-on. Then, the beam-on histogram was normalized, which resulted in a probability density function for the target position during beam-on (PDF_{BO}).

A longitudinal profile of the calculated dose distribution was extracted from the treatment planning system (TPS). To simulate the dosimetric effect of the residual

respiratory motion, the dose profile was convolved by the PDF_{BO} from measurement 1 to 6.

The dose profiles measured using film contained a background dose received from fluoroscopic imaging. This background was removed by subtracting a constant value such that the measured dose matched the convolved calculated dose. Then, the calculated and the convolved dose profile were compared with dose profiles from the measurements using a 1-D gamma analysis (3%/2 mm, 10% low dose threshold).

2.4 | Modeling of dosimetric effects in clinical data

From all patients treated with lung SBRT in expiration gating, we selected five from whom RTR was able to successfully track the tumor during a substantial part of a fraction. From these patients, who all granted permission to use their data for research purposes, the tumor amplitude was measured on the 4DCT-scan, and the average breathing period and its standard deviation were derived from the waveform that was registered during 4DCT-scan acquisition. Also, we determined the distance between the caudal edge of the ITV and the caudal edge of the GTV in the 50% phase bin. Further details on tumor location and treatment techniques are provided in the supplementary materials, Table S1 and Figure S2.

The RTR data acquired during the treatment was visually inspected, and data points showing discontinuities that could not be assigned to actual tumor motion were rejected. Then, for each arc where RTR data was available, a PDF_{BO} was derived. Since most tumor motion was in a longitudinal direction, and the coplanar treatment causes the steepest dose gradients in longitudinal direction, we chose to focus on the analysis of longitudinal motion effects. For all individual treatment arcs of one treatment fraction, the calculated longitudinal dose profiles were exported from the TPS and convolved with PDF_{BO} to assess the effects of residual motion on the delivered dose distribution. For arcs without usable RTR data, we used the PDF_{BO} from the precedent arc. Finally, the dose profiles of the individual arcs were summed, resulting in the total convolved dose for the specific treatment fraction. The supplementary materials provide all acquired RTR data and information about which data was rejected (Figure S3). To quantify the impact of the residual motion on the dose coverage of the tumor, the longitudinal shift of the 100% dose level of the caudal side of the profiles was determined. We focus on the caudal side of the tumor since this is the side that moves away from the beam when transitioning to inhale, and thus may potentially suffer underdosage. To assess the effect of breathing speed, the analysis was repeated after manipulating the RTR and RPM signals' time-axes such that breathing frequency was increased to 2 s per cycle. Furthermore, to simulate the effect of gating systems with larger latency values, the simulations were also repeated using a latency value of 500 ms which was achieved by shifting the beam-on signals.

3 | RESULTS

3.1 | Measurements and simulations

For phantom experiments 1–4, the tracked longitudinal position of the sphere is plotted along with the recorded RPM signal in Figure 1. The intervals where the beam was turned on by the gating system are marked. In experiment 4, we observed that for a motion pattern with a varying period, using phase gating, the RPM system was not able to correctly detect the phase at all times and therefore inconsistently turned the beam off and on. This resulted in a gamma pass rate (3%, 2 mm) of 26%, caused by a smearing of the dose gradients by more than 2 mm toward the inhale position. When using amplitude gating, the beam-on intervals were consistent with the breathing period. For a total of 116 beam transitions, an average delay of 50 ms was observed with an SD of 10 ms between the moment the RPM signal intersects the amplitude threshold and the subsequent change of beam status. Two of these transitions are shown in close-up in Figure 1. We did not observe a difference in delay for beam transitions going from beam-on to off or vice versa.

The measured, calculated, and convolved longitudinal dose profiles are shown in Figure 2 together with the corresponding gamma pass rates. Measurements 4, 5, and 6 showed a smearing of the measured dose gradients, which resulted in decreased gamma pass rates. Measurement 5 not only showed a deformed dose distribution but also a relatively large shift of the entire dose profile. Measurement 7, which was performed without gating on a static phantom, had a gamma pass rate of 100%.

3.2 | Patient data

Table 1 shows for all five patients the tumor motion and the average breathing period observed during 4DCT-scan acquisition and the average breathing period and tumor amplitude during treatment which is derived from the RTR data. Patient 1 had a much lower tumor amplitude during treatment than during the 4DCT-scan.

For all patients, a representative part of the observed tumor motion during treatment and the corresponding RPM signal are shown in Figure 3. The motion traces in this figure show that the tumor position and RPM amplitude are more reproducible from period to period at the expiration peaks than at the inhale peaks. During the treatment session of patient 1, the baseline of the

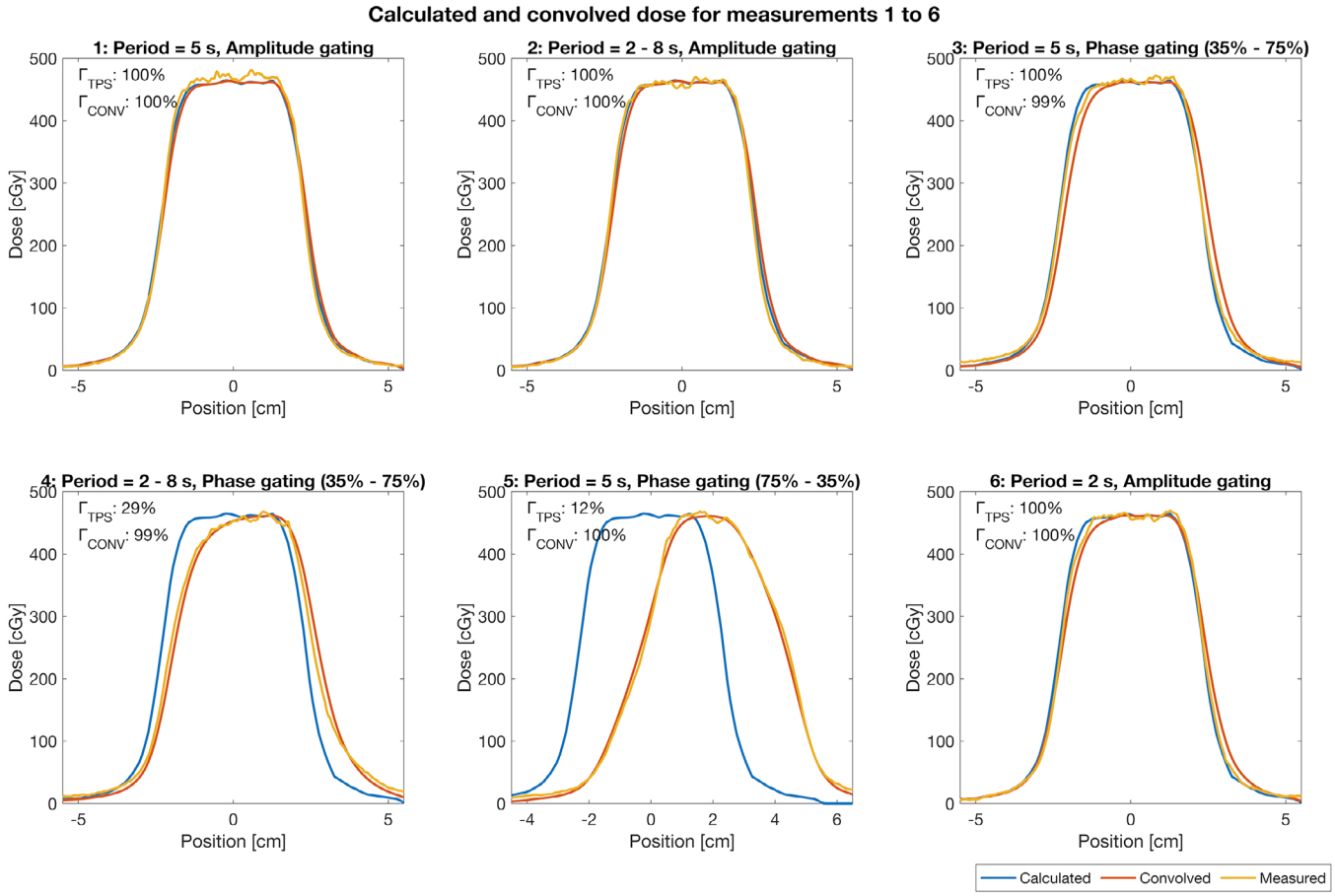

FIGURE 2 Measured, calculated, and convolved longitudinal dose profiles and corresponding gamma pass rates (Γ) from our experiments using the motion phantom. Measurements 1 and 2 were performed using amplitude gating and a regular and irregular motion pattern respectively. In measurements 3 and 4, we used phase gating for regular and irregular motion. Measurement 5 was performed using inverted phase thresholds; in measurement 6, we used amplitude gating for breathing with a short period of 2 s.

TABLE 1 Observed tumor amplitude and breathing period with their standard deviation (SD) for the selected patients.

Patient	Tumor amplitude 4DCT (mm)	Tumor amplitude RTR (SD) (mm)	Breathing period 4DCT (SD) (s)	Breathing period RTR (SD) (s)	ITV to GTV (mm)	100% dose shift at caudal target side (mm) ($T_{original}$ / $T_{2\ seconds}$)	
						L = 50 ms	L = 500 ms
1	19.0	9.9 (1.0)	3.8 (0.6)	3.3 (0.4)	3.5	2.4/2.5	3.9/6.0
2	11.0	13.4 (0.9)	6.7 (0.9)	7.2 (0.8)	3.0	0.6/1.5	1.5/8.3
3	13.1	15.1 (2.9)	3.1 (0.3)	3.4 (0.5)	2.8	0.8/0.9	7.0/9.9
4	11.0	10.8 (2.5)	6.1 (0.6)	4.8 (0.6)	6.5	1.5/1.6	2.8/5.7
5	7.1	7.6 (1.0)	3.9 (0.4)	3.3 (0.3)	3.5	0.0/0.0	0.4/2.2

Distance between the caudal side of ITV and caudal side of the GTV (ITV to GTV). Dose shift at the caudal target side for simulations using two latency values (L) for both the original and the accelerated breathing period ($T_{original}$ and $T_{2\ seconds}$, respectively). A positive shift represents a shift of the dose in cranial direction relative to the tumor.

RPM signal had drifted below "0" from the start of arc 3 (out of four) which caused the beam-on window to shift away from the expiration position. Figure 3 shows the tumor position and RPM signal of the first arc, before the drifting occurred, and the motion data from the first part of the final arc. The final arc was interrupted after the drift was observed. Then, the drift was mitigated by re-learning the RPM signal. Figure 4 shows a PDF for all patients. For patient 1, we show the PDF for the first arc, and for the third arc, where the shift of the beam-on part toward the inhale position is visible. The PDFs for the remaining arcs are provided in the supplementary

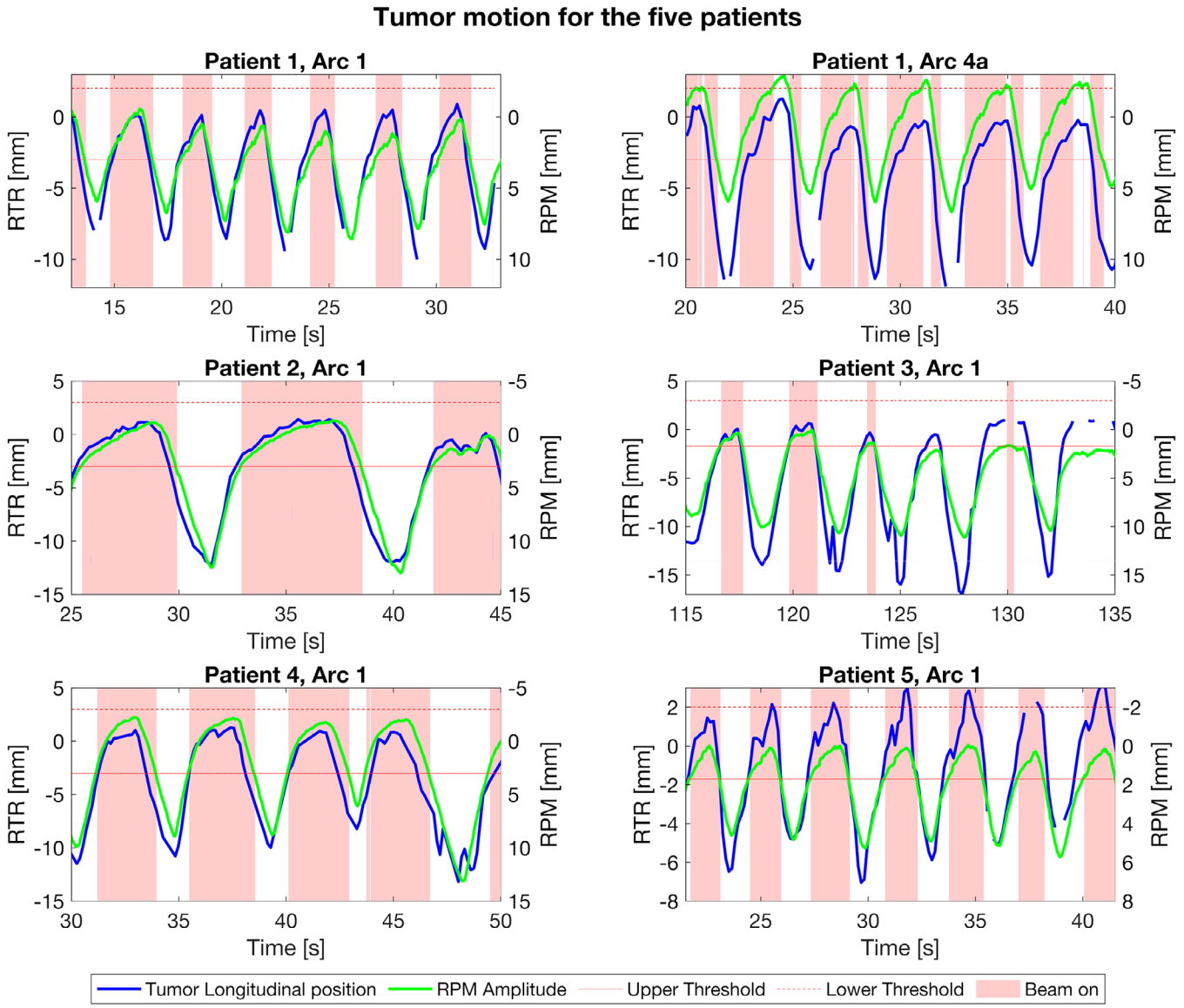

FIGURE 3 Part of the motion traces for five patients. The tumor position tracked by rapid track real-time (RTR), the corresponding real-time position management (RPM) signal. Beam-on intervals are marked in red.

materials (Figure S3). The PDF from patient 3 shows that the beam was off while the tumor was within the treatment window for a substantial portion of time. This observation is supported by Figure 3, where the RPM seems to have a small baseline shift causing it not to return entirely to "0," causing a less efficient gating window. For all patients, the PDF_{BO} shows a tail toward the inhale position. These tails show that the beam was on during a portion of the time that the tumor was not at expiration position, incidentally when the tumor was moving out of the caudal side of the ITV (See Figure 5).

Relative to the tumor, the dose envelope is shifted in the cranial direction, which might result in underdosing of the caudal tumor edge. The observed dose shift at the caudal edges of the target volume is reported in Table 1. Without added extra latency, the dose shift was hardly affected by the breathing speed. For patients 1 to 4, the dose distribution shifted in cranial direction. For patient 5, we observed a dose shift of 1.5 mm on the cranial side of the target. Both Figures 3 and 4 show that for this patient, the tumor position was on average 2 mm too far in the cranial direction. For all patients, stronger dependency on breathing speed was observed for the higher latency of 500 ms.

4 | DISCUSSION

In this study, we determined the dosimetric effect of residual intra-fraction tumor motion for patients that

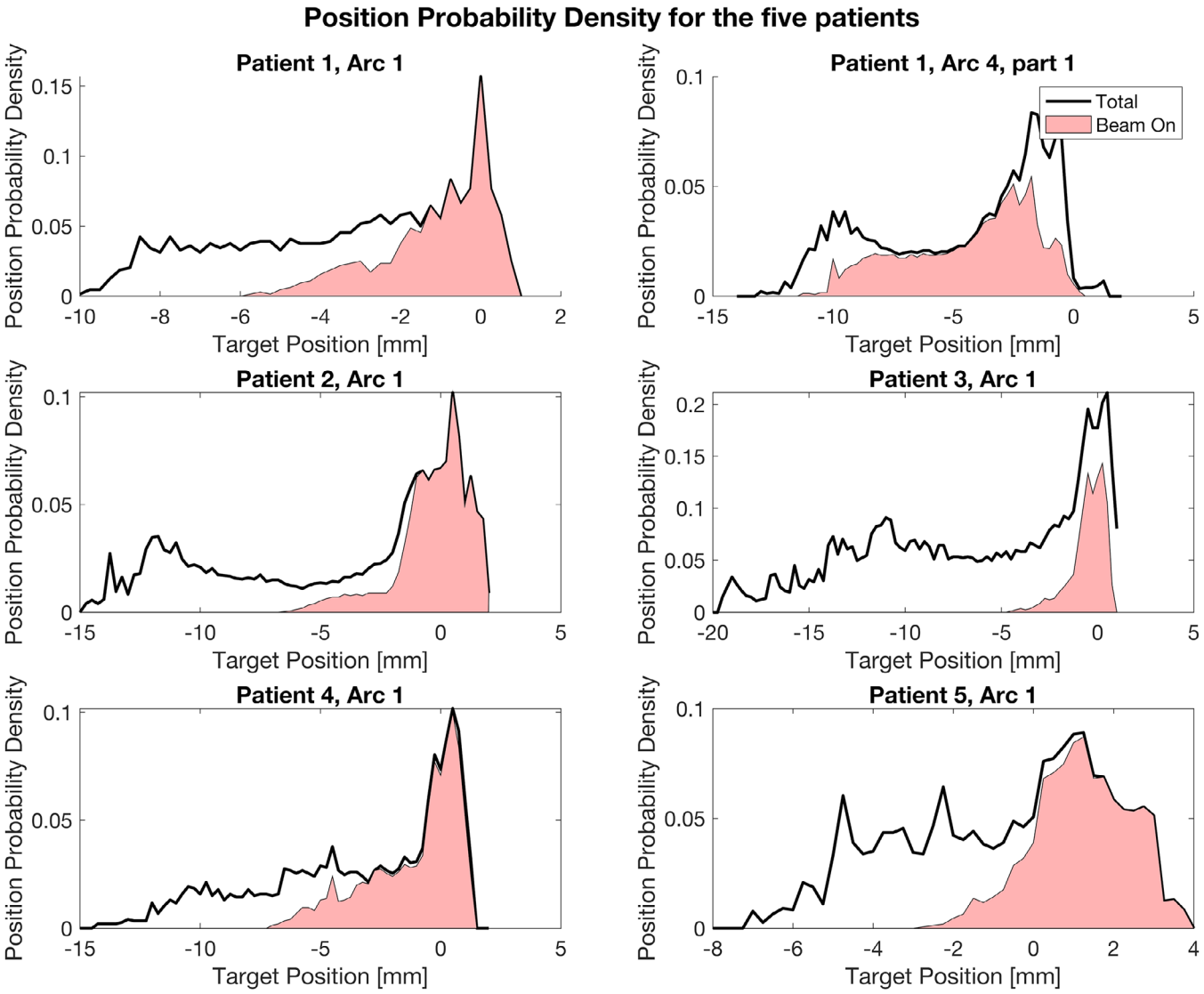

FIGURE 4 Probability density functions (PDF) for five patients, showing the beam-on portion in red. Target position of 0 mm is around exhalation (cranial), negative position is toward inhalation (caudal).

were treated with lung SBRT in expiration gating by means of phantom measurements and simulations based on actual patient data. By combining the recorded respiratory signal with real-time tumor position tracked using RTR, we were able to accurately predict the results of measurement on the respiratory motion phantom. For a latency of 50 ms, which is reported in literature for the RPM system, the dosimetric shift was < 1.5 mm for four patients, while it was 2.4 mm for one patient where an RPM baseline drift of 2 mm occurred which had not been noticed during treatment. This baseline drift caused a shift of the upper-and lower gating threshold toward the inhale position, which resulted in excessive tumor motion within the gating window. The results demonstrated that expiration gating is a safe technique and short periods of larger tumor position deviations up to 7 mm, for example, motion toward the inhale position within the gating latency period, did not result in substantial dosimetric deviations. Nonetheless, it is sensitive to changes in baseline position.

4.1 | Measurements and simulations

In phantom measurement 7, in the absence of target motion, an excellent agreement between calculated and measured dose was found. Therefore, we conclude that dose calculation on the QUASAR phantom is accurate.

For motion patterns with a regular period, both phase- and amplitude gating performed well and lead to a high agreement between measured and calculated dose. However, if the motion has varying periods, the gating system is not able to correctly determine the actual phase of the breathing pattern in real-time,

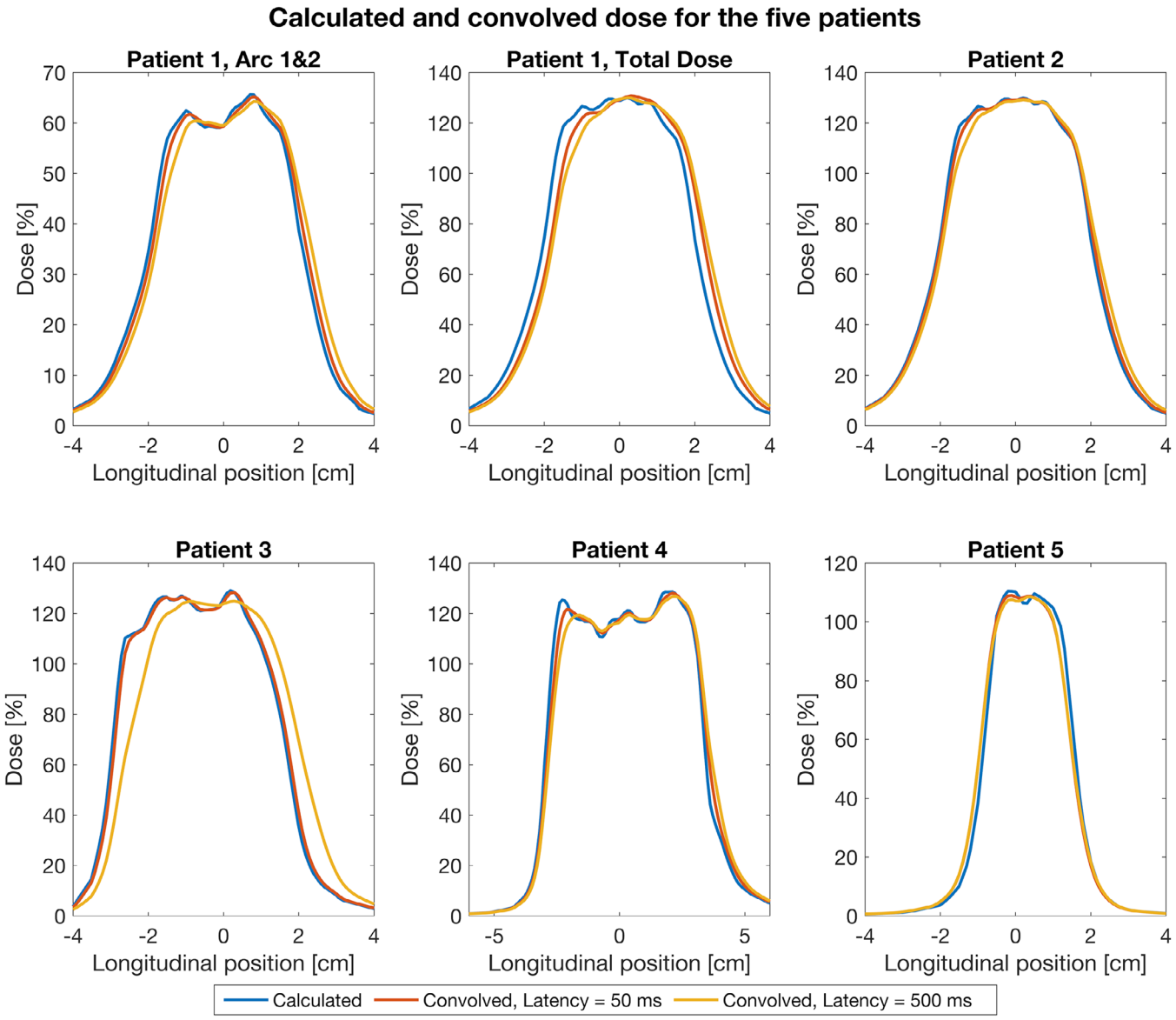

FIGURE 5 Longitudinal dose profiles through the isocenter for patients 1 to 5, overlayed by the profiles convolved by the probability density function for different latency values.

which resulted in incorrect beam-on intervals and measured dose deviating substantially from the TPS calculated dose. This confirms the findings in a previous publication[27] that amplitude gating is more accurate. For amplitude gating, the dose distribution was not affected by the irregularity of the breathing pattern.

The observed apparent gating latency of 50 ms in our RPM data closely resembles the beam-off latency values for the RPM system as reported in literature, which range from 44 to 58 ms.[15,30] Therefore, for the measurements, there was no need to further manipulate the beam-on intervals for incorporating latency in simulations for the RPM system.

For all measurements, we found an excellent agreement between the measured and the convolved dose distribution, even in experiments where the dose distribution was heavily deformed or displaced like experiments 4 and 5. Therefore, we conclude that PDF_{BO} convolution gives a good estimation of the dosimetric effect of residual intra-fraction motion.

4.2 | Patient data

For all patients, the observed dose shift was within the ITV to GTV distance and therefore the tumor received the full prescribed dose, even in the case where there was a baseline drift of the RPM signal, and even though there are no separate amplitude thresholds for going into expiration and subsequently returning to inhale.

RTR directly tracks the actual position of the tumor itself and based on this, we believe that the tumor volume was fully covered with the prescribed dose almost all of the time. The dose shift of patient 5 was in the opposite direction compared to the other patients, which was confirmed by the more cranial tumor position in Figures 3 and 4. Since the online match that was performed on the gated CBCT prior to treatment was found to be correct, the observed shift might have been caused by a patient movement between positioning and the start of treatment.

Based on the observed dose shifts for these five patients, we cannot conclude that the modeled dose shift was larger for patients with a shorter breathing period. However, when manipulating the tumor motion data such that a breathing period of 2 s is simulated, for each individual patient, a shorter breathing period causes a larger shift toward inhale position. Neither can we conclude that the dose shift for tumors with a larger amplitude was larger than those with a small motion amplitude, given the latency that is reported for the RPM system. However, when simulating a larger latency value such as reported for SGRT systems,[16,17] the dose shifts occasionally exceeds the ITV to GTV distance and then might also consume a substantial portion of the PTV margin. Special measures should be taken when using devices with high latency values, for example, by regulating the breathing speed using coaching in order to prevent short breathing periods.

For patient 1, we observed a 2 mm drift in the RPM signal, whilst RTR showed that the tumor returned to "0" in expiration. It happens that re-learning of the RGSC baseline, followed by a verification CBCT-scan, had been omitted. In this particular case, the effect of the RPM drift could have been mitigated by the application of phase gating. However, if the tumor position drifts away from its original position together with the RPM signal, it might be more likely that this shift is overlooked when using phase gating. For this patient, we also observed that the tumor amplitude during acquisition of the 4DCT-scan was much larger than observed during treatment. Therefore, irradiation of the entire tumor trajectory would have led to unnecessary irradiation of healthy lung tissue.

A drift of the RPM signal was also observed during treatment of patient 3. In this case, it only led to unnecessary short gating windows elongating the overall treatment time, but it had no dosimetric consequence for the 50 ms latency situation. It is important to pay attention to the RPM signal during treatment. However, it should be realized that the surface is only a surrogate, and the relation between the surface and the tumor position is not always stable. The surface position can be influenced by, for example, muscle tension in the back (e.g., due to stress), bowel motion, muscle tension in the abdomen, changing from abdominal breathing to partly thoracic breathing. Real-time information about the actual tumor position could further improve safety and might eventually lead to redundancy of the RPM signal when direct tumor tracking is possible.

4.3 | Limitation

The convolution-based model that we used to simulate the dosimetric effects of residual motion is not time resolved. At best, we were able to perform the convolution arc-by-arc using patient-specific RTR data. Our method ignores intra-fraction interplay effects which are shown to be small in previous studies.[31–33] In earlier work, Riley (2014) already concluded that the accumulated target dose can be substantially impaired for patients who show a large amount of variation in breathing speed and amplitude. They state that a limit at which respiratory irregularity disqualifies a patient for gated treatment must be determined. Although we believe that amplitude gating might be a better option for these patients, the convolution method that we used might be useful to determine optimal and safe patient-tailored gating settings. Our analysis is performed in a single longitudinal dose profile, ignoring motion in other directions. This represented the dominant motion trajectory in these, and in most, cases. If necessary, and with sufficient RTR data, the analysis could be expanded. Another limitation is that the method we have used requires actual data of the tumor position in time. This was obtained using non-clinical software (RTR), which we realize is not widely available. Furthermore, we have only tested this method for five patients. The RTR method is now based on template matching, and we have previously shown[9,34] that this method only works if the tumors are sufficiently visible on the kV images, meaning that the method cannot be used for all patients. However, recent developments in deep learning for tumor position monitoring[35] show promising results in terms of a higher tracking rate and more accurate tracking.

5 | CONCLUSION

Using film measurements in a respiratory motion phantom, we showed that amplitude gating is robust for irregular breathing patterns. Using data derived from real-time tracking of the tumor position, we demonstrated that for the five patients, expiration gating was a dosimetrically accurate method of treatment delivery since the tumor position is reproducible in expiration. For all observed treatment fractions, the dosimetric shift caused by tumor motion within the gating window is smaller than the ITV to GTV distance at the caudal side when using gating systems with a low latency. During delivery, attention is needed to react in a timely manner to respiratory drift. When using gating systems with a large latency value, one should be aware of the

dosimetric consequences and consider measures to regularize breathing.

ACKNOWLEDGMENTS

The RTR research software was provided by Varian Medical Systems.

CONFLICT OF INTEREST STATEMENT

The department has research collaborations with Varian Medical Systems. Verbakel is employed by both Varian and the Amsterdam UMC since May 2023. Verbakel received honoraria for meetings and lectures. Hoffmans, Remmerts de Vries, and Dahele have no conflicts of interest.

DATA AVAILABILITY STATEMENT

The data used in this study is available upon request.

REFERENCES

1. Keall PJ, Mageras GS, Balter JM, et al. The Management of Respiratory Motion in Radiation Oncology Report of AAPM Task Group 76. Vol 33. 2006. doi:10.1118/1.2349696
2. Ball HJ, Santanam L, Senan S, Tanyi JA, van Herk M, Keall PJ. Results from the AAPM Task Group 324 respiratory motion management in radiation oncology survey. *J Appl Clin Med Phys*. 2022;23(11):1-11. doi:10.1002/acm2.13810
3. Hazelaar C, van der Weide L, Mostafavi H, Slotman BJ, Verbakel WFAR, Dahele M. Feasibility of markerless 3D position monitoring of the central airways using kilovoltage projection images: managing the risks of central lung stereotactic radiotherapy. *Radiother Oncol*. 2018;129(2):234-241. doi:10.1016/j.radonc.2018.08.007
4. Zeng C, Lu W, Reyngold M, et al. Intrafractional accuracy and efficiency of a surface imaging system for deep inspiration breath hold during ablative gastrointestinal cancer treatment. *J Appl Clin Med Phys*. 2022;23(11):1-9. doi:10.1002/acm2.13740
5. Saito T, Sakamoto T, Oya N. Comparison of gating around end-expiration and end-inspiration in radiotherapy for lung cancer. *Radiother Oncol*. 2009;93(3):430-435. doi:10.1016/j.radonc.2009.09.002
6. Oh SA, Yea JW, Kim SK, Park JW. Optimal gating window for respiratory-gated radiotherapy with real-time position management and respiration guiding system for liver cancer treatment. *Sci Rep*. 2019;9(1):1-6. doi:10.1038/s41598-019-40858-2
7. Oh SA, Yea JW, Kim SK. Statistical determination of the gating windows for respiratory-gated radiotherapy using a visible guiding system. *PLoS One*. 2016;11(5):1-12. doi:10.1371/journal.pone.0156357
8. Hazelaar C, Dahele M, Mostafavi H, Van Der Weide L, Slotman B, Verbakel W. Markerless positional verification using template matching and triangulation of kV images acquired during irradiation for lung tumors treated in breath-hold. *Phys Med Biol*. 2018;63(11). doi:10.1088/1361-6560/aac1a9
9. Remmerts de Vries IF, Dahele M, Mostafavi H, Slotman B, Verbakel W. Markerless 3D tumor tracking during single-fraction free-breathing 10MV flattening-filter-free stereotactic lung radiotherapy. *Radiother Oncol*. 2021;164:6-12. doi:10.1016/j.radonc.2021.08.025
10. Malinowski K, McAvoy TJ, George R, Dietrich S, D'Souza WD. Incidence of changes in respiration-induced tumor motion and its relationship with respiratory surrogates during individual treatment fractions. *Int J Radiat Oncol Biol Phys*. 2012;82(5):1665-1673. doi:10.1016/j.ijrobp.2011.02.048
11. Takao S, Miyamoto N, Matsuura T, et al. Intrafractional baseline shift or drift of lung tumor motion during gated radiation therapy with a real-time tumor-tracking system. *Int J Radiat Oncol Biol Phys*. 2016;94(1):172-180. doi:10.1016/j.ijrobp.2015.09.024
12. Nishioka S, Nishioka T, Kawahara M, et al. Exhale fluctuation in respiratory-gated radiotherapy of the lung: a pitfall of respiratory gating shown in a synchronized internal/external marker recording study. *Radiother Oncol*. 2008;86(1):69-76. doi:10.1016/j.radonc.2007.11.014
13. Shepard AJ, Matrosic CK, Radtke JL, Jupitz SA, Culberson WS, Bednarz BP. Technical Note: characterization of clinical linear accelerator triggering latency for motion management system development. *Med Phys*. 2018;45(11):4816-4821. doi:10.1002/mp.13191
14. Chugh B, Smith W. SU-E-T-120: measurement of time delays in gated radiotherapy for realistic breath motions. *Med Phys*. 2013;40(6):231. doi:10.1118/1.4814555
15. Worm ES, Thomsen JB, Johansen JG, Poulsen PR. A simple method to measure the gating latencies in photon and proton based radiotherapy using a scintillating crystal. *Med Phys*. 2023;50(6):3289-3298. doi:10.1002/mp.16418
16. Wiersma RD, McCabe BP, Belcher AH, Jensen PJ, Smith B, Aydogan B. Technical note: high temporal resolution characterization of gating response time. *Med Phys*. 2016;43(6):2802-2806. doi:10.1118/1.4948500
17. Barfield G, Burton EW, Stoddart J, Metwaly M, Cawley MG. Quality assurance of gating response times for surface guided motion management treatment delivery using an electronic portal imaging detector. *Phys Med Biol*. 2019;64(12). doi:10.1088/1361-6560/ab205a
18. Lujan AE, Larsen EE, Balter JM, Ten Haken RK. A method for incorporating organ motion due to breathing into 3D. *Med Phys*. 1999;26(5):715-720. doi:10.1118/1.1609057
19. Chetty IJ, Rosu M, Tyagi N, et al. A fluence convolution method to account for respiratory motion in three-dimensional dose calculations of the liver: a Monte Carlo study. *Med Phys*. 2003;30(7):1776-1780. doi:10.1118/1.1581412
20. Kelly A, Williams M, Metcalfe P. A predictive method of calculating the dosimetric effect of 1-D motion on narrow multileaf collimated segments. *Australas Phys Eng Sci Med*. 2009;32(1):1-10. doi:10.1007/BF03178621
21. Poulsen PR, Schmidt ML, Keall P, Worm ES, Fledelius W, Hoffmann L. A method of dose reconstruction for moving targets compatible with dynamic treatments. *Med Phys*. 2012;39(10):6237-6246. doi:10.1118/1.4754297
22. Skouboe S, Poulsen PR, Muurholm CG, et al. Simulated real-time dose reconstruction for moving tumors in stereotactic liver radiotherapy. *Med Phys*. 2019;46(11):4738-4748. doi:10.1002/mp.13792
23. Skouboe S, Ravkilde T, Bertholet J, et al. First clinical real-time motion-including tumor dose reconstruction during radiotherapy delivery. *Radiother Oncol*. 2019;139:66-71. doi:10.1016/j.radonc.2019.07.007
24. Li HS, Chetty IJ, Enke CA, et al. Dosimetric consequences of intrafraction prostate motion. *Int J Radiat Oncol Biol Phys*. 2008;71(3):801-812. doi:10.1016/j.ijrobp.2007.10.049
25. Poulsen PR, Worm ES, Petersen JBB, Grau C, Fledelius W, Høyer M. Kilovoltage intrafraction motion monitoring and target dose reconstruction for stereotactic volumetric modulated arc therapy of tumors in the liver. *Radiother Oncol*. 2014;111(3):424-430. doi:10.1016/j.radonc.2014.05.007
26. Saito T, Matsuyama T, Toya R, et al. Respiratory gating during stereotactic body radiotherapy for lung cancer reduces tumor position variability. *PLoS One*. 2014;9(11):1-6. doi:10.1371/journal.pone.0112824
27. Lee M, Yoon KJ, Cho B, et al. Comparing phase- and amplitude-gated volumetric modulated arc therapy for stereotactic body

radiation therapy using 3D printed lung phantom. *J Appl Clin Med Phys*. 2019;20(2):107-113. doi:10.1002/acm2.12533
28. Nakamura M, Narita Y, Sawada A, et al. Impact of motion velocity on four-dimensional target volumes: a phantom study. *Med Phys*. 2009;36(5):1610-1617. doi:10.1118/1.3110073
29. Publicover J, Vandermeer A, Norrlinger B, Alasti H. SU-GG-T-305: feasibility of using a programmable respiratory motion phantom for QA and assessment of dosimetric implications of breathing motion during radiation therapy. *Med Phys*. 2008;35(6Part14):2795. doi:10.1118/1.2962057
30. Lempart M, Kügele M, Ambolt L, Blad B, Nordström F. Latency characterization of gated radiotherapy treatment beams using a PIN diode circuit. *Irbm*. 2016;37(3):144-151. doi:10.1016/j.irbm.2016.02.002
31. Ong C, Verbakel WFAR, Cuijpers JP, Slotman BJ, Senan S. Dosimetric impact of interplay effect on RapidArc lung stereotactic treatment delivery. *Int J Radiat Oncol Biol Phys*. 2011;79(1):305-311. doi:10.1016/j.ijrobp.2010.02.059
32. Riley C, Yang Y, Li T, Zhang Y, Heron DE, Huq MS. Dosimetric evaluation of the interplay effect in respiratory-gated RapidArc radiation therapy. *Med Phys*. 2014;41(1). doi:10.1118/1.4855956
33. Ong CL, Dahele M, Slotman BJ, Verbakel WFAR. Dosimetric impact of the interplay effect during stereotactic lung radiation therapy delivery using flattening filter-free beams and volumetric modulated arc therapy. *Int J Radiat Oncol Biol Phys*. 2013;86(4):743-748. doi:10.1016/j.ijrobp.2013.03.038
34. de Bruin K, Dahele M, Mostafavi H, Slotman BJ, Verbakel WFAR. Markerless real-time 3-dimensional kV tracking of lung tumors during free breathing stereotactic radiation therapy. *Adv Radiat Oncol*. 2021;6(4):100705. doi:10.1016/j.adro.2021.100705
35. Grama D, Dahele M, van Rooij W, Slotman B, Gupta DK, Verbakel WFAR. Deep learning-based markerless lung tumor tracking in stereotactic radiotherapy using Siamese networks. *Med Phys*. 2023;50(11):6881-6893. doi:10.1002/mp.16470

SUPPORTING INFORMATION

Additional supporting information can be found online in the Supporting Information section at the end of this article.

How to cite this article: Hoffmans D, Remmerts de Vries I, Dahele M, Verbakel W. Quantifying the dosimetric accuracy of expiration-gated stereotactic lung radiotherapy. *Med Phys*. 2025;52:2773–2784. https://doi.org/10.1002/mp.17743